Supplementary Materials for

Universal Theory and Basic Rules of Strain-Dependent Doping Behaviors in Semiconductors

Xiaolan Yan[1], Pei Li[1], Su-Huai Wei[1,2], and Bing Huang[1,2]

[1] *Beijing Computational Science Research Center, Beijing 100193, China*
[2] *Department of Physics, Beijing Normal University, Beijing 100875, China*

List of Content

strain η. (b) a-$\varepsilon^{0/-1}(\eta)$ of Mg_{Al} as a function of strain η. Band edge positions are fixed at the values of unstrained AlN.

Part I: Method for defect calculations.

All the density functional theory (DFT) calculations are performed with Vienna Ab Initio Simulation Package (VASP) [1]. The exchange-correlation energy is treated using the generalized gradient approximation (GGA) in the PBE form [2]. The hybrid functional (HSE06) is adopted to correct the bandgaps of semiconductors [3]. The plane-wave cutoff energy is set to 520 eV and sufficient *k*-mesh are selected for all the systems. During the structural relaxations, a conjugate-gradient algorithm is used until the force on each atom was lower than 0.01 eV $Å^{-1}$, and the total energy is converged to 1.0×10^{-6} eV. For the defect calculations, the standard supercell approach is adopted [4, 5].

The formation energy (H_f) of a defect or dopant in semiconductors can be evaluated as [4, 6-8]

$$H_f^{D,q}(V, E_F) = E_t^{D,q}(V) - E_t^{host}(V) + \sum n_i\mu_i + qE_F \quad (1),$$

where $E_t^{host}(V)$ is the total energy of the supercell without a defect, and $E_t^{D,q}(V)$ is the total energy of a supercell with a defect in a charge state q. q is the number of electrons transferred from the supercell to the reservoirs in forming the defect cell and n_i is the number of atoms removed from or added into the supercell and μ_i is the chemical potential of atom i with respect to elemental solid/gas with energy E_i. E_F is the Fermi level.

For the defect calculation, sufficiently large supercell sizes have been adopted and we have tested our results using the different sizes of supercells and confirmed that our main conclusions maintain (see **Fig. 2** and **Figs. S1-S5**). For the strain calculations, the hydrostatic strain is considered in the main text, and our conclusion maintains for the biaxial strain based on our test calculations (see **Fig. S6**).

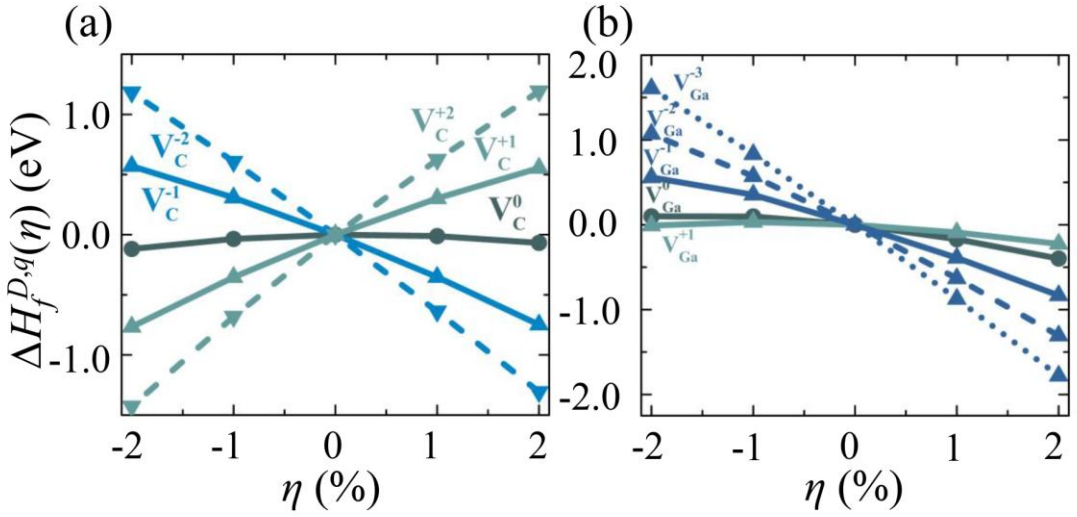

Fig. S1. (a) Change of formation energies $\Delta H_f^{D,q}(\eta)$ for C vacancy (V_C) in SiC as a function of strain η. (b) same for (a) but for Ga vacancy (V_{Ga}) in GaN.

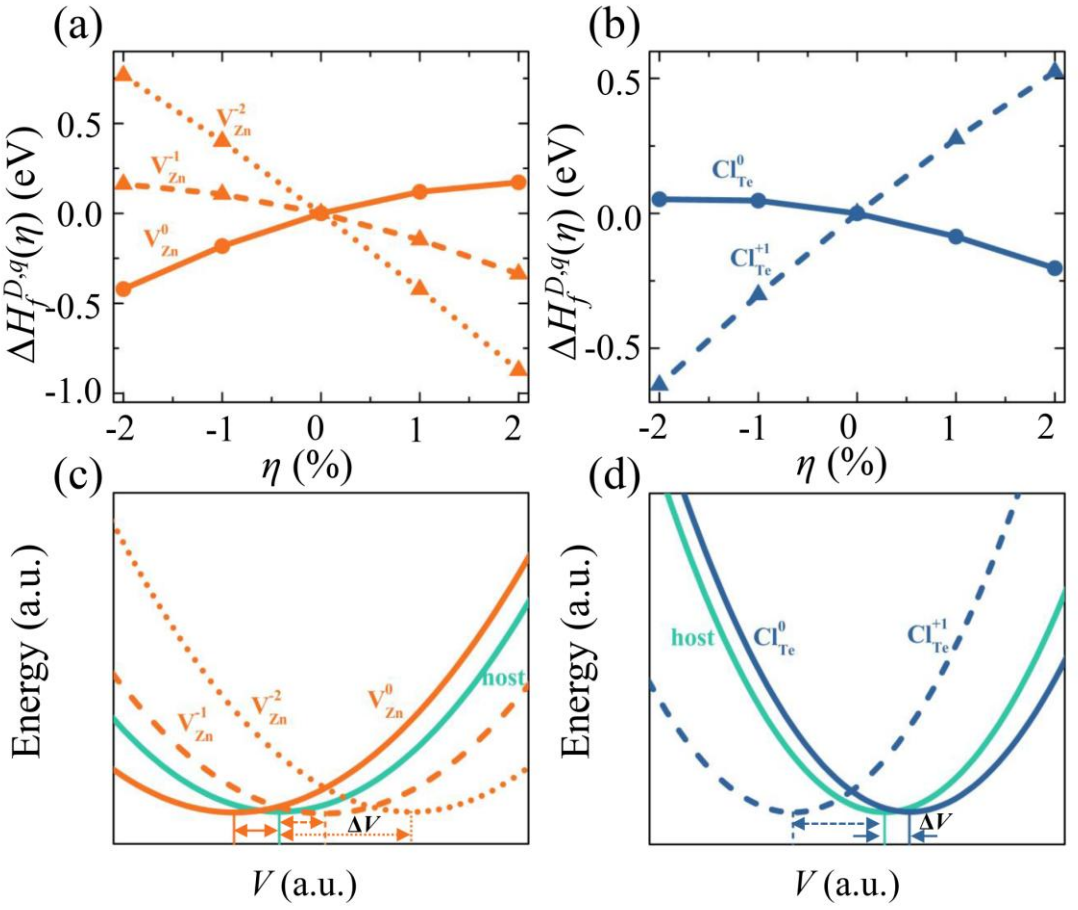

Fig. S2. (a) Change of formation energies $\Delta H_f^{D,q}(\eta)$ for Zn vacancy (V_{Zn}) in ZnTe as a function of strain η. (b) same for (a) but for *n*-type (Cl_{Te}) dopant in ZnTe. Schematic plotting of total energies $E_t^{D,q}(V)$ as a function of volume V for (c) V_{Zn} and (d) Cl_{Te}. $E_t^{host}(V)$ for host are also shown in (c)-(d) for comparison.

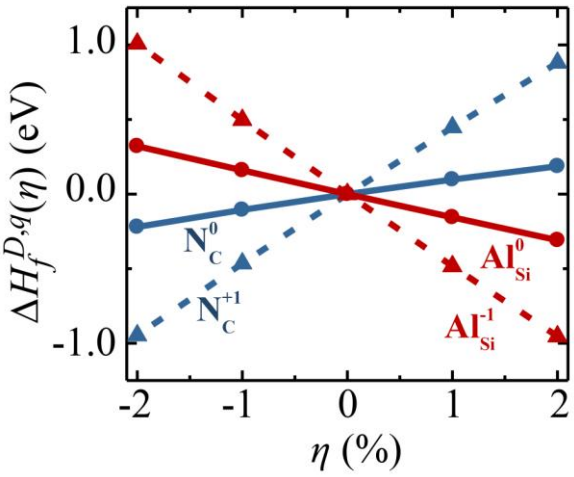

Fig. S3. Change of formation energies $\Delta H_f^{D,q}(\eta)$ for *n*-type (N_C) and *p*-type (Al_{Si}) dopants in SiC as a function of strain η.

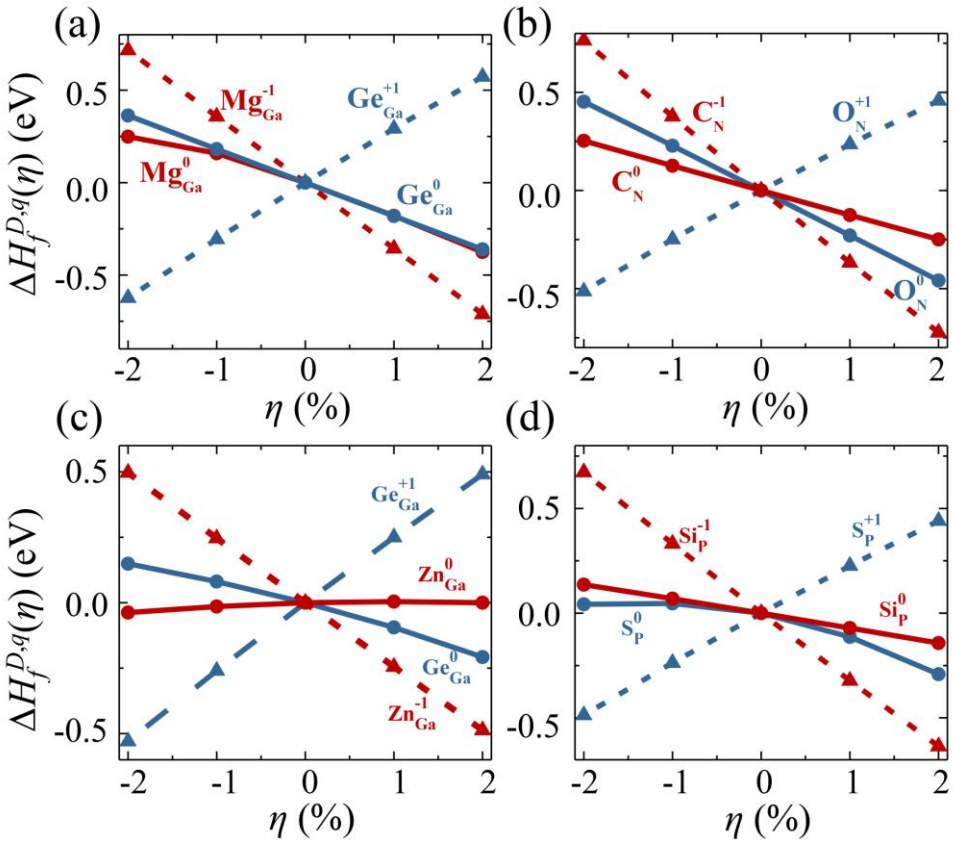

Fig. S4. (a) Change of formation energies $\Delta H_f^{D,q}(\eta)$ for *n*-type Ge_{Ga} and *p*-type Mg_{Ga} in GaN. (b) same for (a) but for *n*-type O_N and *p*-type C_N in GaN. (c) same for (a) but for *n*-type Ge_{Ga} and *p*-type Zn_{Ga} in GaP. (d) same for (a) but for *n*-type S_P and *p*-type Si_P in GaP.

Figure S4 also indicates that the trends are independent of the substitution positions either at anion or cation sites.

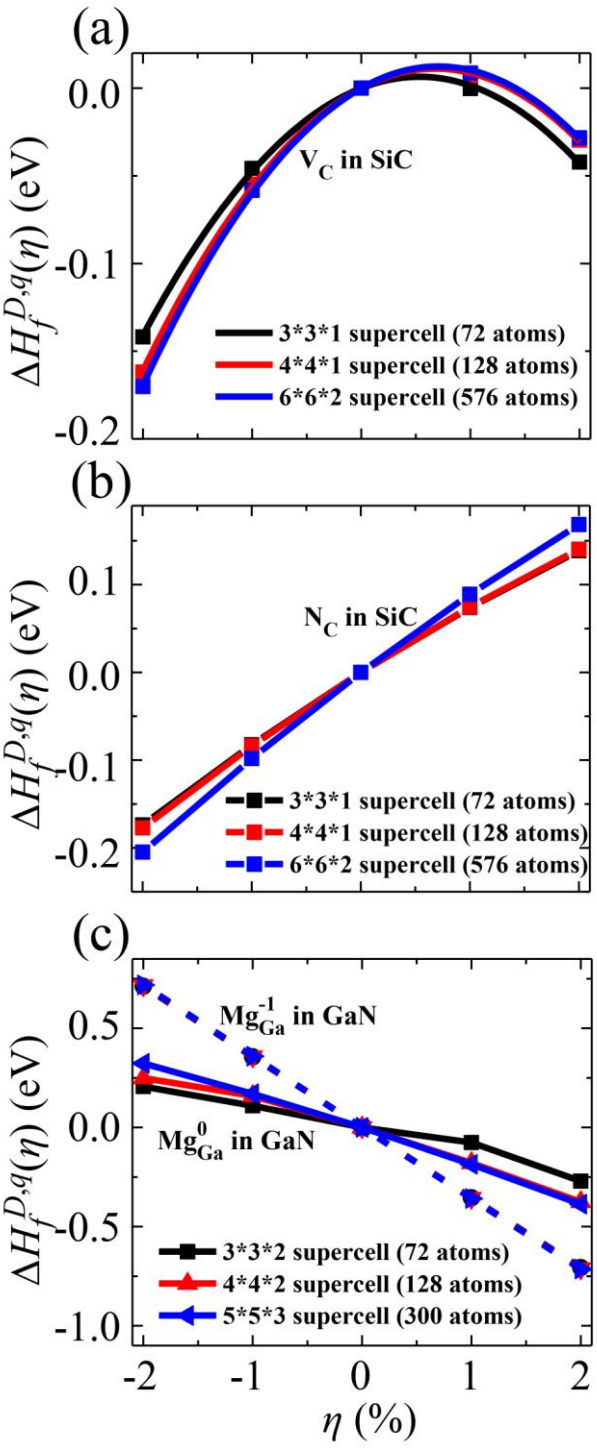

Fig. S5. Change of formation energies $\Delta H_f^{D,q}(\eta)$ for (a) V_C and (b) N_C in 4H-SiC with different supercell sizes, corresponding to different defect concentrations, under strain η. (c) Similar to (b) but for Mg_{Ga} dopants in both q=0 and q=-1 states in GaN.

Figure S5 indicates that the trends of $\Delta H_f^{D,q}(\eta)$ in different semiconductors is independent of the sizes of supercell calculations.

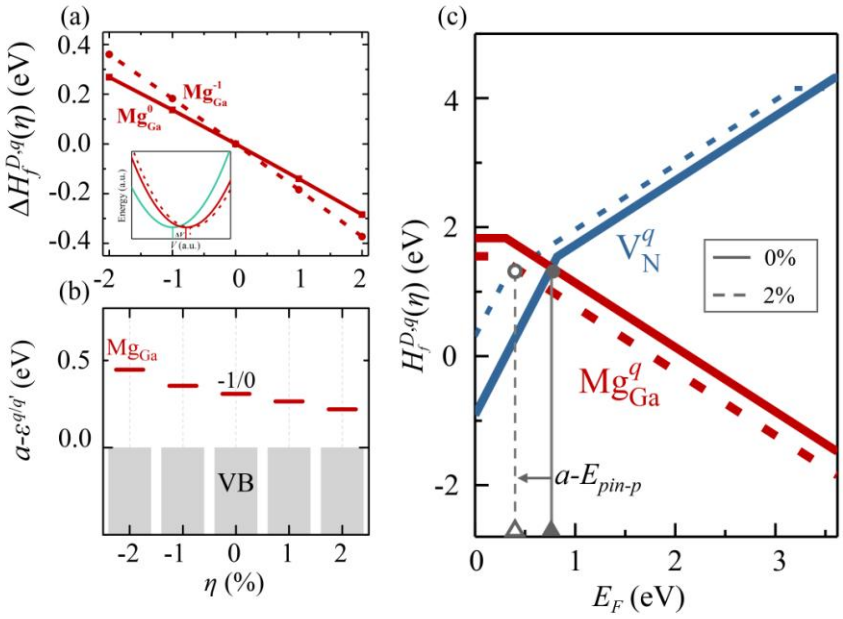

Fig. S6. (a) Change of formation energies $\Delta H_f^{D,q}(\eta)$ for Mg_{Ga} in GaN as a function of biaxial strain η. Inset: Schematic plotting of total energies $E_t^{D,q}(V)$ as a function of volume V for Mg_{Ga}, $E_t^{host}(V)$ for host is also shown for comparison. (b) a-$\varepsilon^{0/-1}(\eta)$ of Mg_{Ga} as a function of biaxial strain η. Band edge positions are fixed at the values of unstrained GaN. (c) Formation energies of external Mg_{Ga} and intrinsic compensating V_N in GaN without and with a +2% biaxial strain.

It indicates that the Rule Nos. I-III are valid for both uniform strain and biaxial strain.

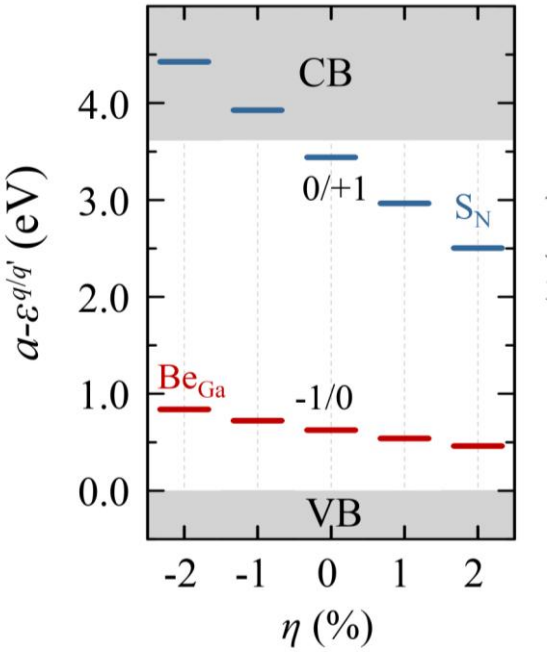

Fig. S7. a-$\varepsilon^{0/-1}(\eta)$ [a-$\varepsilon^{0/+1}(\eta)$] of Be_{Ga} (S_N) in GaN as a function of strain η. Band edge positions are fixed at the values of unstrained GaN.

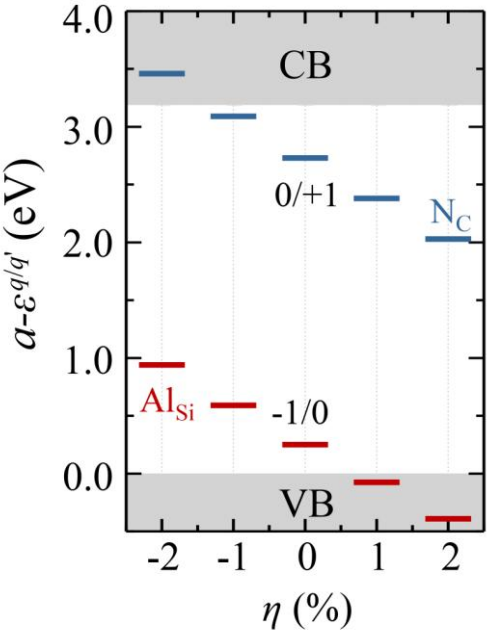

Fig. S8. a-$\varepsilon^{0/-1}(\eta)$ [a-$\varepsilon^{0/+1}(\eta)$] of Al_{Si} (N_C) in SiC as a function of strain η. Band edge positions are fixed at the values of unstrained SiC.

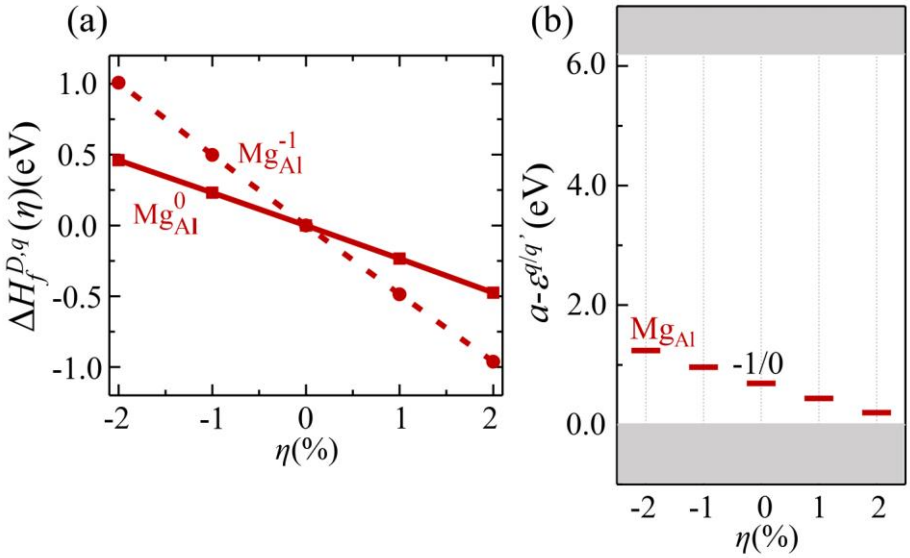

Fig. S9. (a) Change of formation energies $\Delta H_f^{D,q}(\eta)$ for Mg_{Al} in AlN as a function of strain η. (b) a-$\varepsilon^{0/-1}(\eta)$ of Mg_{Al} as a function of strain η. Band edge positions are fixed at the values of unstrained AlN.

References

[1] Kresse G, Furthmuller J 1996 *Phys. Rev. B Condens Matter* **54** 11169.

[2] Perdew J P, Burke K, Ernzerhof M 1996 *Phys. Rev. Lett.* **77** 3865.

[3] Heyd J, Scuseria G E 2003 *J. Chem. Phys.* **118** 8207.

[4] Wei S-H 2004 *Comput. Mater. Sci.* **30** 337.

[5] Freysoldt C, Neugebauer J, Van de Walle C G *Advanced Calculations for Defects in Materials:*
Electronic Structure Methods, (Wiley-VCH Verlag GmbH & Co. KGaA, 2011).

[6] Zhang S B, Northrup J E 1991 *Phys. Rev. Lett.* **67** 2339.

[7] Laks D B, Van de Walle C G, Neumark G F, *et al.* 1992 *Phys. Rev. B Condens Matter* **45** 10965.

[8] Freysoldt C, Grabowski B, Hickel T, *et al.* 2014 *Rev. Mod. Phys.* **86** 253.